Optimization of Unidirectional Carbon/Epoxy Facesheets for Enhanced Flexural Strength in PVC Foam Sandwich Beam

Jameer Havaldar[1], Sachin Shinde[2], Sachin Solanke[1,*], Bhagwan Jogi[1], Pankaj Jadhav[1], Niyati Raut[3]

[1]Department of General Engineering, Institute of Chemical Technology, Matunga East, Mumbai 400 019, India
[2]Department of Mechanical Engineering, Datta Meghe College of Engineering, Airoli, Navi Mumbai 400078, India
[3]Department of Mechanical Engineering, VIVA Institute of Technology, Virar, India

*Author to whom correspondence should be addressed:
E-mail: sg.solanke@ictmumbai.edu.in

(Received June 14, 2025; Revised October 14, 2025; Accepted December 01, 2025)

Abstract: Sandwich composites are lightweight structures comprising stiff, thin face sheets often carbon or glass fibers bonded to a low-density core, delivering high strength-to-weight ratios, superior bending stiffness, and excellent energy absorption. These properties make them ideal for aerospace, automotive, and marine applications. Their performance hinges on core material selection, face sheet composition, and interfacial bonding, prompting research into optimized designs for improved mechanical behavior. This study explores the flexural performance of carbon fiber-reinforced polymer matrix composite sandwich beams by optimizing face sheet configurations. Sandwich panels were fabricated via vacuum infusion, using a Poly-vinyl Chloride (PVC) foam core and varying carbon fibers/epoxy face sheet stacking sequences 2/2, 2/4-, and 4/2-layers top/bottom in the transverse direction. Four-point bending test assessed stiffness, load capacity, and failure mechanisms. The asymmetric 4-top/2-bottom arrangement demonstrated the highest average flexural strength of 6.52 MPa, emphasizing the top layer's role in resisting tensile stresses and enhancing energy dissipation. Material characterization included Differential Scanning Calorimetry (DSC), Fourier Transform Infrared Spectroscopy (FT-IR), Scanning Electron Microscopy (SEM) and Energy-Dispersive X-ray Spectroscopy (EDS). DSC confirmed complete epoxy curing, while FTIR identified key functional groups. SEM revealed fiber rupture and matrix cracking as primary failure modes, with EDS detecting high carbon content, minor oxidation, and chlorine traces from the PVC core. Force-deflection and strain analyses showed asymmetric configurations exhibited more progressive, damage-tolerant failure compared to brittle symmetric sandwich composites. These findings offer critical insights into layer distribution effects, guiding the design of high-performance sandwich composites for structural applications.

Keywords: Carbon Fiber; Epoxy; Poly-Vinyl Chloride (PVC) foam; Scanning Electron Microscope;4-Point bending test

1. Introduction

Polymer matrix composite (PMC) sandwich are advanced structural components that offer a unique combination of high strength, low weight, and excellent mechanical performance[1–3]. These beams are primarily used in industries such as aerospace, automotive, marine, and civil engineering, where the need for efficient weight management without compromising strength is crucial[4–6]. The concept of a sandwich beam involves a three-layer structure: two thin outer skins and a thicker core material between them. The core material plays a vital role in resisting shear forces and enhancing the beam's overall bending stiffness, while the skins bear the external loads and provide resistance to normal stresses[7–9]. The combination of these components allows sandwich beams to maintain impressive mechanical properties while minimizing weight[10–12]. Applications where mass reduction is paramount. For example, in aircraft fuselages and wing structures, sandwich beams with carbon fiber-reinforced polymer (CFRP) skins and a Nomex

Cite: J. Havaldar et al., "Optimization of Unidirectional Carbon/Epoxy Facesheets for Enhanced Flexural Strength in PVC Foam Sandwich Beam". Evergreen, 13 (01) 307-327 (2026). https://doi.org/10.5109/7411077.

honeycomb core are widely used. These components reduce overall aircraft weight while maintaining high strength and stiffness, contributing to improved fuel efficiency and performance[13–16]. In automotive industries high-performance sports cars often use sandwich panels with glass fiber skins and foam cores in doors, hoods, and floors. These panels help lower the vehicle's weight, enhancing acceleration, fuel economy, and handling without compromising safety[17–20]. The skins of a polymer matrix composite sandwich beam are typically made from high-performance composite materials. These are often constructed from polymer resins reinforced with fibers, such as carbon, glass, or aramid fibers. These fibers offer exceptional strength and stiffness, while the resin matrix binds them together, creating a solid, durable structure[21,22]. The primary objective is to create a lightweight, high-strength, and high-stiffness composite material. The carbon fiber face sheets provide excellent tensile strength and stiffness, while the PVC foam core offers low density and high shear resistance, resulting in a structure with a superior strength-to-weight ratio. Sandwich structures are often favoured over traditional materials due to their excellent corrosion resistance[23–26]. Thanks to their numerous benefits, these composite systems have found widespread application in the automotive, aerospace, marine, and various industrial sectors[27–31]. They have also attracted increasing interest in the construction industry and are beginning to be adopted for civil engineering purposes For example, sandwich panels with concrete face sheets and a lightweight foam or honeycomb core are increasingly used in bridge decks and prefabricated building panels[32,33]. These allow for faster installation and reduce the load on the foundation while maintaining load-bearing capacityCompared to concrete panels, these structures are considerably lighter[34]. The use of GFRP (glass fiber reinforced polymer) sandwich panels in building construction dates back to the 1970s[35]. The fundamental design principle of sandwich structures is that the face sheets (skins) are responsible for bearing in-plane tensile and compressive stresses resulting from bending, while the lightweight core maintains the separation between the skins and transmits shear forces to the supports[36–38]. The fundamental design principle of sandwich structures lies in the division of mechanical responsibilities between the face sheets and the core[39–44]. The face sheets, typically made from strong composite materials, resist in-plane tensile and compressive stresses caused by bending one skin stretches while the other compresses[45–49]. Meanwhile, the lightweight core, although not very strong on its own, plays a crucial role by maintaining the distance between the face sheets and transmitting shear forces across the structure to the supports[50,51]. This separation significantly increases the beam’s bending stiffness without adding much weight, making sandwich structures ideal for high-performance applications where both strength and lightness are essential[26]. Numerous studies have investigated the flexural behaviour and failure mechanisms of composite sandwich structures[52–54]. In past literatures, Russo et al. carried out the four point bending test in accordance with ASTM C 393-62 in which the span length of sandwich panel with PVC core and Polyester core was 330mm and the thickness and width was 16mm and 75mm respectively. The ultimate load that this sandwich structure got was 1500N for structure with PVC core and got 1100 N of ultimate force for structure containing polyester foam. Jameer et al carried out the four point bending test in accordance with ASTM D 5467with carbon fibers and PVC foam as core material, in which the span length of the sandwich panel was 210mm. the thickness and width was 29mm and 25mm respectively. The ultimate load that this sandwich structure got was 910N[44]. S Mudassir et al. carried out four point bending test in accordance with ASTM D 7250 in which the span length of the sandwich composite with polyurethane and phenolic core was 200mm and thickness and width was 25mm and 75mm respectively. The ultimate load that this sandwich panel sustained before breaking was 7kN for Polyurethane foam and 6kN for phenolic foam. Jameer et al carried out the four point bending test in accordance with ASTM D 5467 in which the span length of the sandwich panel was 210mm. the thickness and width was 29mm and 25mm respectively. The ultimate load that this sandwich structure got was 910N with PVC core[42]. Q. Chen et al carried out four point bending test of sandwich panel consisting of PVC foam and Glass fibers. The test was carried out in accordance with ASTM D 7250 in which the span length of sandwich composite was 180mm and thickness was 10mm with width of 75mm. The ultimate load that the sandwich panel got was around 600 N. Jameer et al. carried out four point bending test in accordance with ASTM D5467 with carbon fibers and PVC foam as core materials, in which the span length of the sandwich panel was 210mm. the thickness and width was 29mm and 25mm respectively. The ultimate load that this sandwich structure got was 910N[41].

The study focuses on novelty of the fabrication, flexural testing and characterization of carbon fiber-reinforced sandwich composites with PVC cores, manufactured using the vacuum infusion process. The research explores the effects of varying layer configurations (e.g., 2/2, 2/4, and 4/2 layers at top/bottom) on the flexural performance of these composites under transverse loading conditions.

The investigation includes comprehensive mechanical testing, such as 4-point bending tests conducted in accordance with ASTM D 5467[55], to evaluate flexural strength, stiffness, and failure modes. Additionally, advanced analytical techniques like Differential Scanning Calorimetry (DSC), Fourier Transform Infrared Spectroscopy (FT-IR) and Scanning Electron Microscope (SEM) with Energy Dispersive X-Ray Spectroscopy are

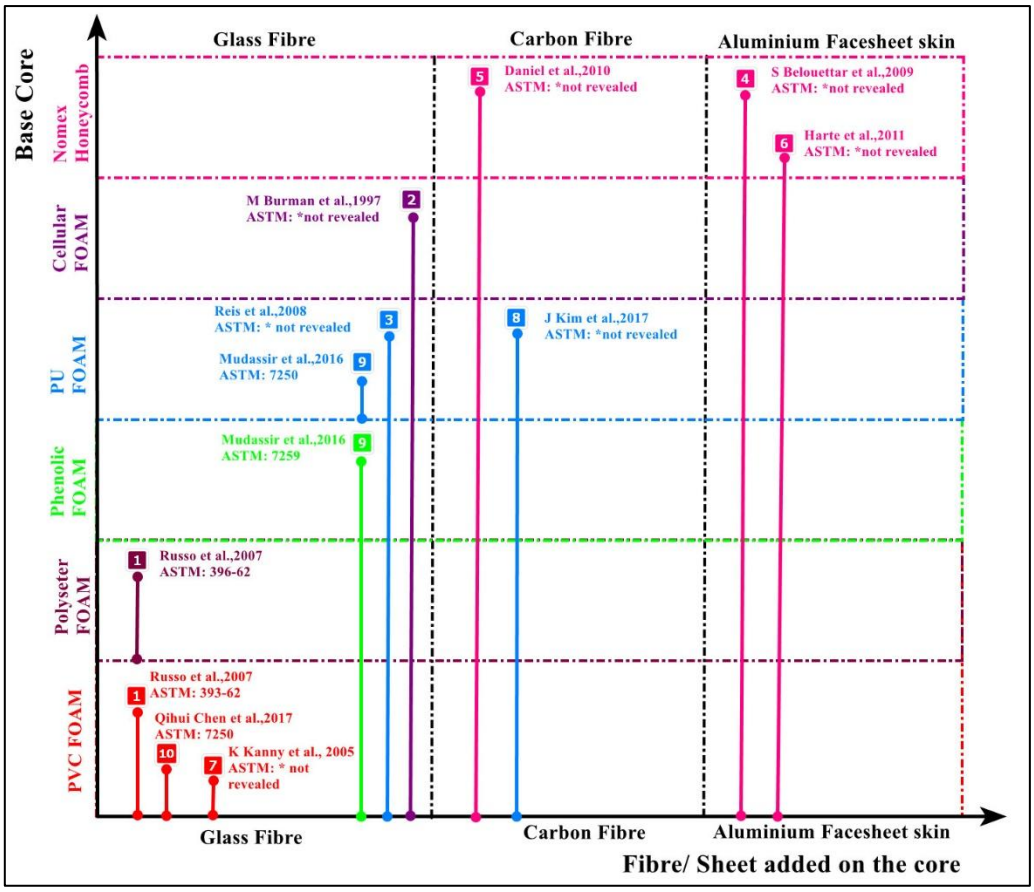

Fig. 1: Novelty of work represented against the work done by earlier researchers

employed to study the thermal curing behaviour, chemical composition of the epoxy resin system, high resolution surface imaging and elemental analysis of material respectively. The DSC analysis provides insights into the glass transition temperature (Tg) and curing kinetics, FT-IR confirms the molecular structure of the cured and uncured resin, while SEM-EDX combines the high magnification imaging capabilities of SEM with elemental analysis provided by EDX. This technique is used in various fields to characterize materials, identify contaminants, and investigate the cause of damage. This work expands upon previous studies by introducing novel material combinations (carbon fiber/epoxy with PVC cores) and advanced fabrication methods (vacuum infusion). The results contribute to a deeper understanding of how layer symmetry and fiber orientation influence mechanical performance, offering valuable data for optimizing composite designs in high-performance applications. The findings are supported by detailed graphical analyses, including force-deflection curves, strain distribution, and visual documentation of failure mechanisms, providing a robust foundation for future research and industrial applications[56].

2. Material Selection

The sandwich panels are made of Carbon fiber/Epoxy skin and Poly-Vinyl Chloride (PVC) foam as a core material of density 60kg/m3 with a core thickness of 25mm which was provided by Fine Finish Industries Pvt Ltd, Taloja. The main advantages of using PVC foam in sandwich composites include its low weight, resistance to moisture and chemicals, ease of fabrication, and ability to withstand high loads and stresses[6,57–59]. Carbon fiber facesheets are used for their exceptionally high specific stiffness and specific strength, meaning they offer superior rigidity and load-bearing capacity for very little weight. This allows the composite to effectively resist tensile and compressive forces from bending loads, while the core material handles shear stresses, maximizing the overall structural efficiency. The carbon face-sheet thickness was of 0.8mm. The facesheet was arranged in transverse direction. Transverse fiber orientation provides strength and stiffness against loads applied perpendicular to the main axis, preventing splitting, improving multi-directional load-bearing capacity along the length of the sandwich composite and reducing weight. The length of the sandwich composite, length of the beam was 210mm and 25mm width respectively in accordance with ASTM D 5467[55]. The sandwich panel was manufactured using the vacuum infusion process[60,61]. This process is an advanced manufacturing technique used to produce high-quality sandwich composite structures. This process employs

vacuum pressure to draw resin into dry reinforcements, ensuring uniform resin distribution and enhanced mechanical properties[62,63].

3. Sample Preparation for Composite Material

The process used for preparation of sample is vacuum infusion which uses a mould made with aluminium. The vacuum infusion process utilizes atmospheric pressure to compact the dry fiber layup and core, ensuring excellent wet-out and minimizing excess resin. This results in a composite with a higher fiber-to-resin ratio, leading to superior mechanical properties, reduced weight, and fewer voids compared to open-molding techniques. Firstly, clean the aluminium mould thoroughly to ensure its free from dust and then apply release agent Poly-vinyl Alcohol (PVA) to mould to prevent sticking, then cut the Carbon fiber fabric to required dimensions (250x220) mm so that at least 5 samples should get from the panel of width 25mm and length 210mm. Similarly cut the PVC core of required dimension as shown in Figure 1. The next step is to lay the peel ply on the aluminum mould and then lay 2 layers of carbon fiber fabric on the mould (bottom facesheet), next place the PVC core on the top of the bottom layer then place 2 layers of carbon fiber fabric over the core, ensure everything is aligned and fits well. The next step is to put the peel ply on top of carbon fiber layer followed by vacuum mesh to ensure that the resin flows throughout the surface evenly and then seal the edges using sealant tape (tacky tape). Ensure there are no leaks in the bag. Connect the Vacuum pump and check the leaks. Place spiral tubing along the sides and edges and cover the entire layup with vacuum bagging film[64]. Next step is to mix the resin system (epoxy resin) with hardener at a ratio of 100:38 by weight, after mixing start the infusion by allowing resin to be sucked by the vacuum from the inlet to outlet as shown in Figure 2. Monitor the flow to avoid dry spots or voids which can hamper the strength of composite. Once the entire layup is fully saturated, clamp off the resin inlet, keep vacuum applied until gelation (initial curing). Allow to fully cure under vacuum for 24 hours at ambient temperature. The 24-hour curing period is necessary to allow for the completion of the polymerization process, where the resin and hardener molecules form extensive cross-linked polymer chains. This extended time ensures the composite reaches its maximum glass transition temperature (Tg) and achieves optimal mechanical properties, such as strength, stiffness, and thermal stability. Once cured, remove the vacuum bag, flow media and peel

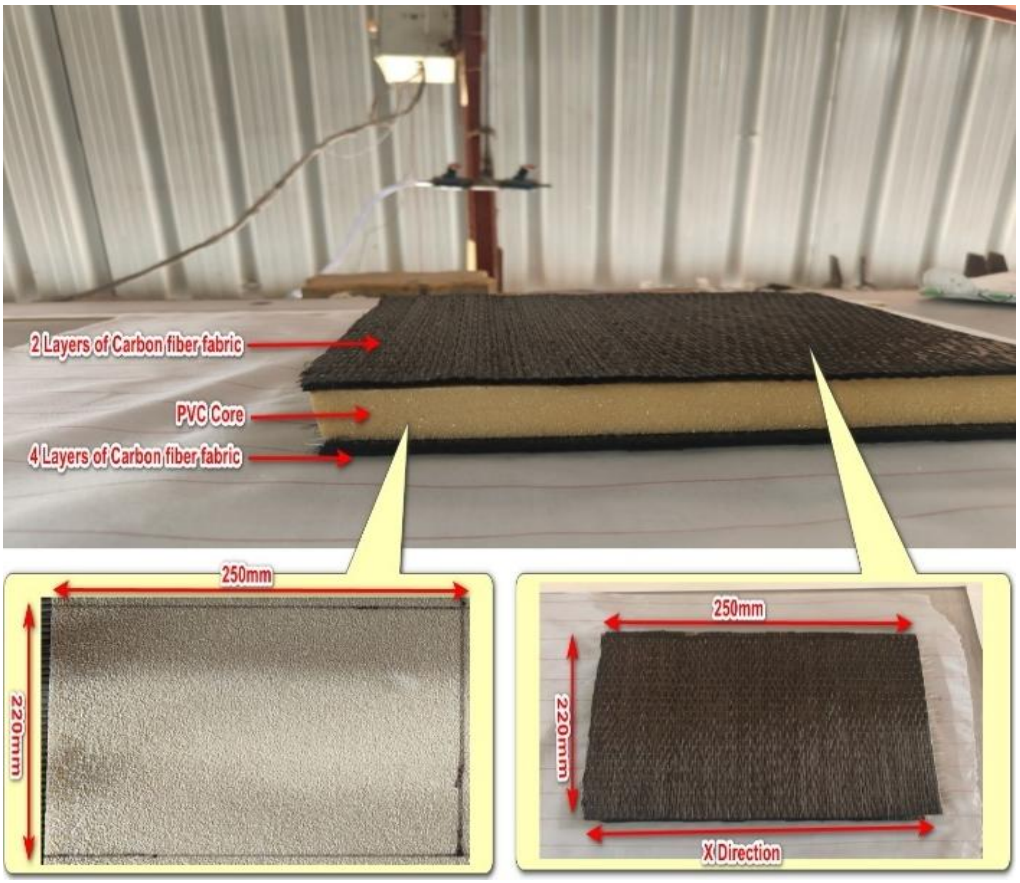

Fig. 2: Carbon fabric and PVC core setup

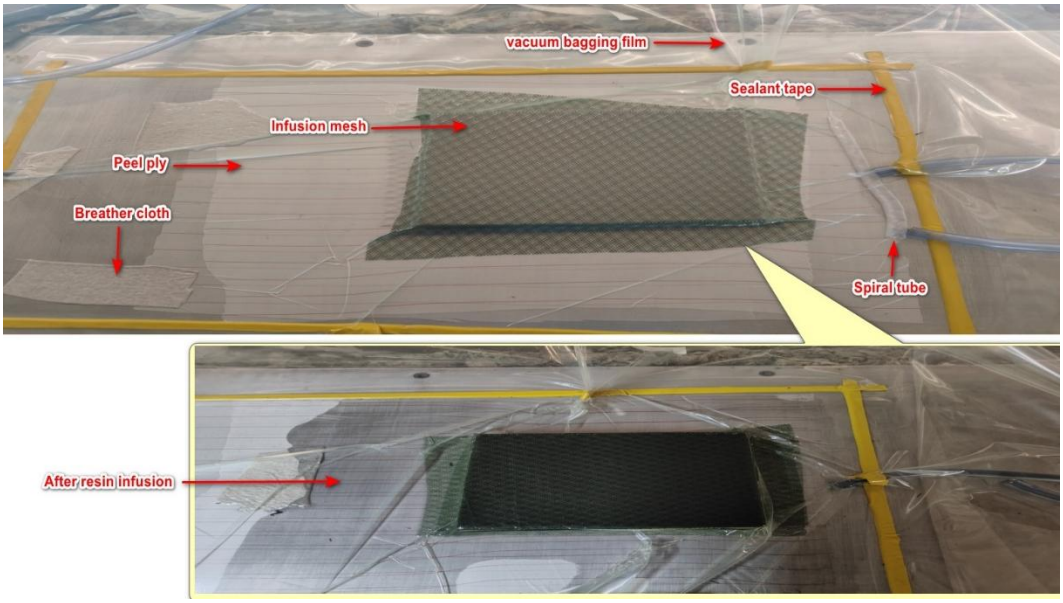

Fig. 3: After applying Vacuum pressure and Epoxy resin

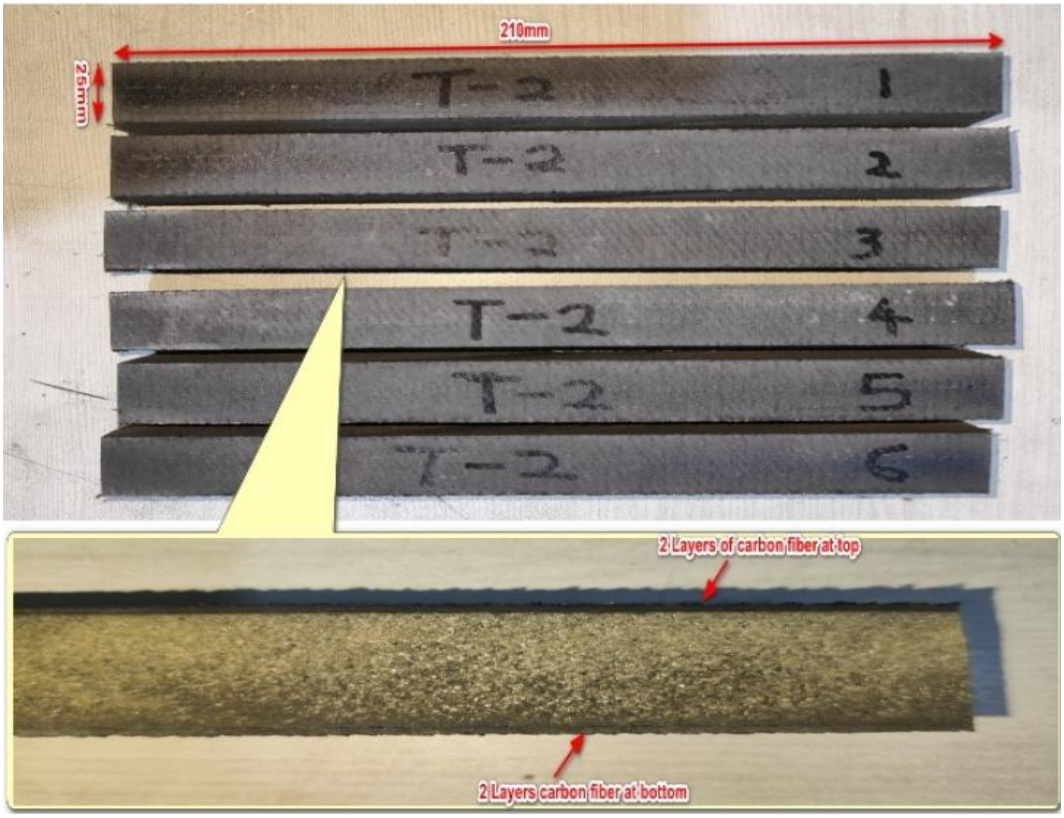

Fig. 4: Composite samples after de-moulding and cutting

ply[65,66]. And then carefully remove the finished composite from the mold. After de-moulding cut the composite panel to 5 to 6 specimens of dimensions 25mm width and 210mm length as per ASTM D 5467 as shown in Figure 3. The same procedure was carried out for all the sandwich panels with different stacking layers at top and bottom i.e. 2 layers of carbon fiber fabric on top and 4 layers of carbon fiber fabric at bottom and. 4 layers of carbon fiber fabric on top and 2 layers of carbon fiber fabric at bottom. Refer Figure 4

4. Results & Discussion

4.1. Flexural test (4-point bending)

The 4-point bending test is ideal for composite materials because it provides a uniform bending moment and reduces shear effects compared to 3-point bending. In sandwich composites, a 4-point bending test is preferred

because it creates a region of uniform maximum bending moment between the two inner loading points, free from shear forces. This provides a more accurate measurement of the material's true flexural properties by avoiding premature failure from stress concentrations that occur under the single central load of a 3-point test. It is widely used in industries requiring high-performance composites to ensure structural reliability. The 4-point bending test is a widely used method for evaluating the flexural performance of composite materials, providing insights into their stiffness, strength, and failure mechanisms under bending loads. In this test, a composite beam is supported at two outer points while two inner points apply a symmetrical load, creating a uniform bending moment between the inner loading points and reducing shear effects. This setup allows for a more accurate assessment of the material's bending behaviour, making it particularly suitable for brittle or layered composites prone to delamination. The test helps identify failure modes such as fiber breakage, matrix cracking, or interfacial debonding. Due to its reliability, the 4-point bending test is commonly employed in industries like aerospace, automotive, and civil engineering to validate the structural integrity of composite components.

The formula for calculating the flexural strength is given by:

$$\sigma_f = 3P(L-a)/2bh^2 \quad (1)$$

Where:

σ_f = Flexural strength (MPa or N/mm²)

P = Maximum applied load (N)

L = Support span (distance between outer supports) (mm)

a = Distance between the inner loading points (mm)

b = Width of the specimen (mm)

h = Thickness (total height) of the specimen (mm)

4.2. Test setup and procedure

The static flexural test of composite sandwich beams was performed in accordance with the ASTM D 5467/ 5467 Mstandard. The load was applied on the quarter point of the span through a 50kN Tinius Olsen universal testing machine with a load cell of 50kN precisely because it measures the applied force on the composite specimen, ensuring accurate flexural strength and stiffness calculations as shown in Figure 5. Its high-resolution data helps detect early failure events and ensures reliable, standardized test results for material validation. The applied load, displacements and strains were recorded and obtained using video extensometer and a data logger system.

4.3. Four point bending result of Carbon fiber reinforced sandwich composite (2 fibre layers at top and 2 fibre layers at bottom) for fibres aligned in transverse direction

In a 4-point bend test, the bottom of the beam experiences the highest tensile (stretching) stress, while the top is under the highest compressive (squashing) stress as shown in Figure 6 and Figure 7. Since most common materials are weaker and more likely to crack under tension than compression, failure typically starts at the bottom.

The graph (Force vs. Deflection by Crosshead) shows a clear elastic rise in force with deflection up to ~600 N as shown in Figure 8, followed by a sudden drop and fluctuations, indicative of brittle fracture and instability post-peak. Overall, the composite displays elastic behaviour up to peak load with abrupt failure, and a well-defined load-bearing capacity consistent with sandwich composite characteristics.

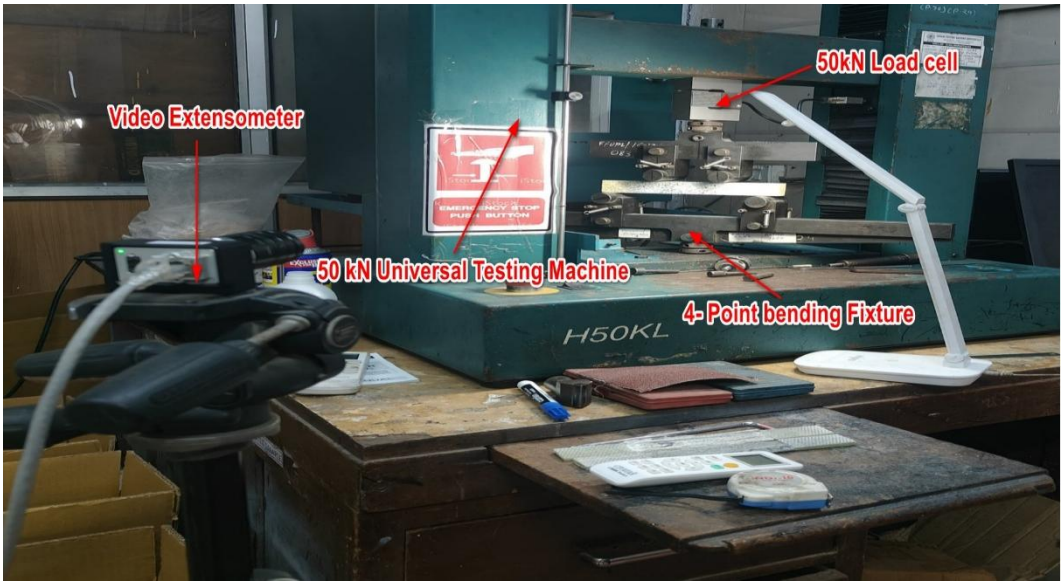

Fig. 5: Overall testing setup

Cite: J. Havaldar et al., "Optimization of Unidirectional Carbon/Epoxy Facesheets for Enhanced Flexural Strength in PVC Foam Sandwich Beam". Evergreen, 13 (01) 307-327 (2026). https://doi.org/10.5109/7411077.

Fig. 6: Breaking point after applying load

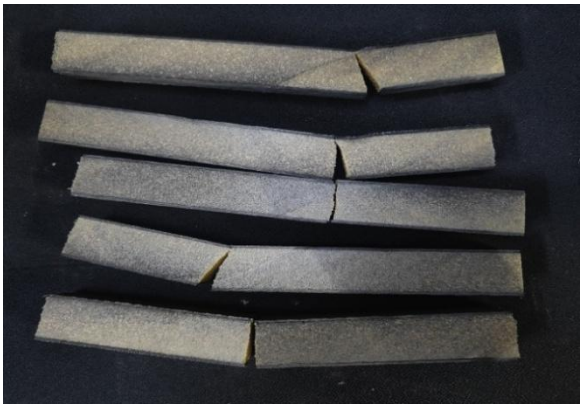

Fig. 7: Specimen broken after loading

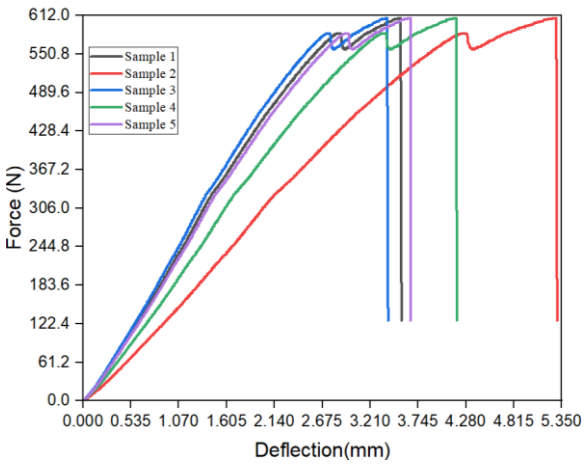

Fig. 8: Force Vs Deflection for Carbon fiber composite (2 Layers at top and 2 layers at bottom)

Figure 9 and 10 shows the ultimate force and flexural strength taken by the 5 samples under consideration for 2 layer at the top and two layers at the bottom design.

4.4. Four point bending result of Carbon fibre reinforced sandwich composite (2 fibre layers at top and 4 fibre layers at bottom) for fibres aligned in transverse direction

The graphs of Figure 10 show the transverse response of

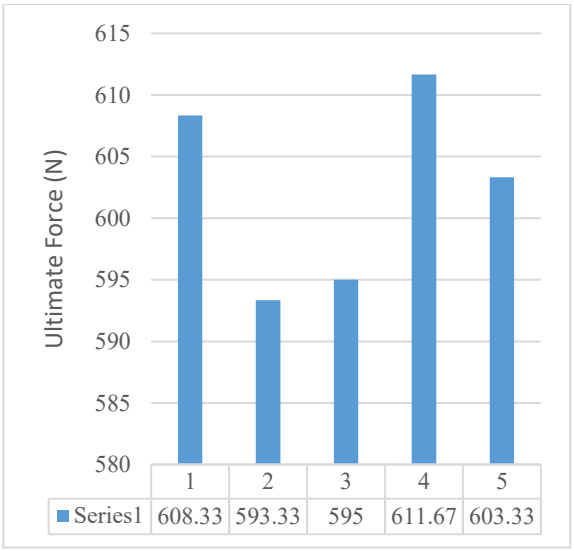

Fig. 9: Ultimate Force 5 Samples of carbon fiber composite (2 Layers at top and 2 layers at bottom

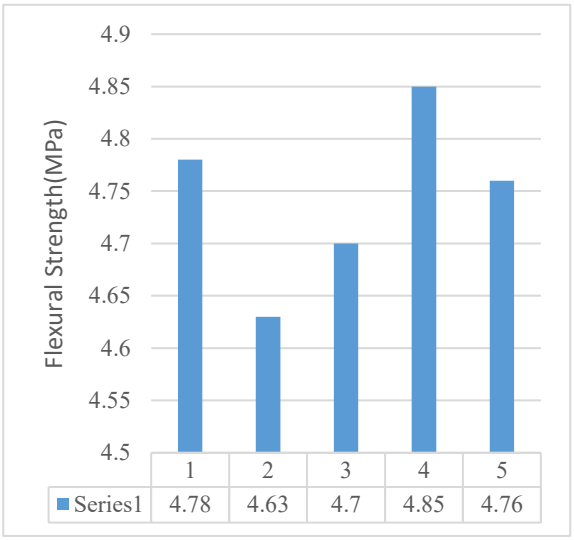

Fig. 10: Flexural strength of all 5 Samples of carbon fiber composite (2 Layers at top and 2 layers at bottom

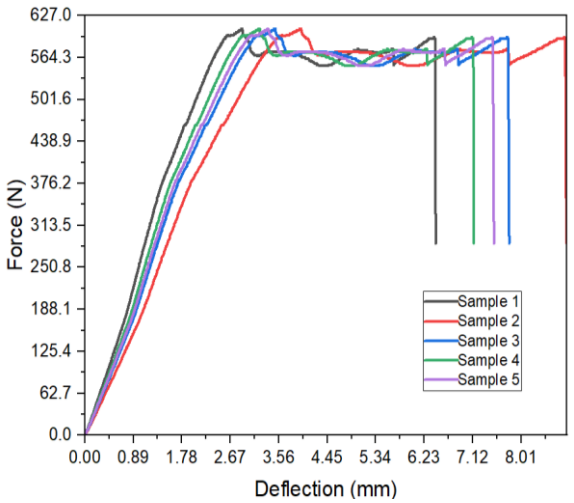

Fig. 11: Force Vs Deflection for Carbon fiber composite (2 Layers at top and 4 layers at bottom)

Fig. 12: Breaking point of carbon fiber (top 2 bottom 4) sandwich composite

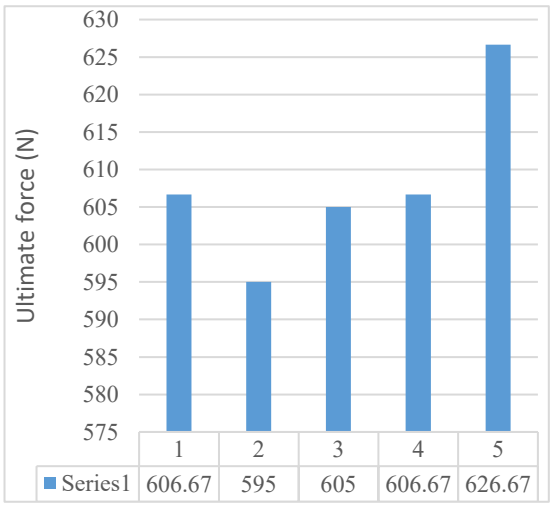

Fig. 13: Ultimate Force of all 5 Samples of carbon fiber composite (2 Layers at top and 4 layers at bottom)

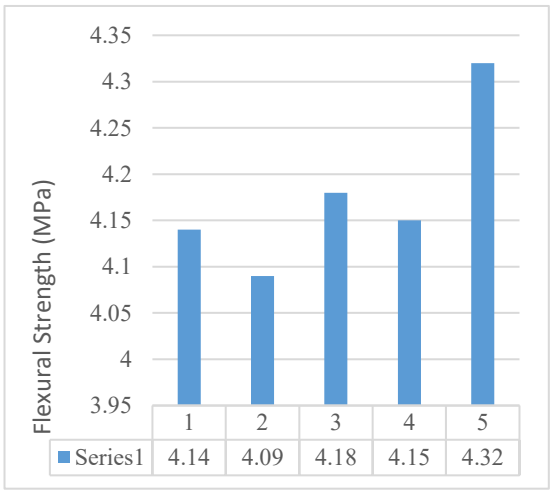

Fig. 14: Flexural strength of all 5 Samples of carbon fiber composite (2 Layers at top and 4 layers at bottom)

carbon fiber composites under 4-point bending, revealing a consistent yet slightly extended deformation behaviour compared to earlier sample.

In the graph (Force vs. Deflection by Crosshead), the load-deflection curve rises sharply and levels off around 626.67 N as shown in Figure 11, followed by fluctuations and delayed failure, indicating a more ductile post-peak response or progressive failure mode. Overall, this sample set demonstrates higher deflection capacity and potential energy absorption before complete failure, with top-facing strain dominating the deformation profile. Figure 12 shows the actual test done on Universal testing machine for 4 Layers at bottom and 2 layers at top whereas Figure 13 shows the Ultimate strength obtained from 5 samples and Figure 14 shows the Flexural strength.

4.5. Four point bending result of Carbon fibre reinforced sandwich composite (4 fibre layers at top and 2 fibre layers at bottom) for fibres aligned in transverse direction

Figure 15 shows the actual test done on Universal testing machine for 4 Layers at top and 2 layers at bottom.

In the graph (Force vs. Deflection by Crosshead), the force-deflection response is strong and consistent, with a gradual and continuous increase in force up to ~910 N as shown in Figure 16. Multiple sharp drops in force indicate sequential failure events like delamination or cracking, but the structure continues to carry load after each, suggesting good damage tolerance. The overall higher force and deflection range compared to previous tests reflect improved mechanical performance.

Figure 17 and Figure 18 show ultimate force and Flexural strength for 4 Layers at top and 2 layers at bottom design.

Figure 19 shows the average ultimate force for all the three combinations whereas Figure 20 shows average flexural strength of all the designs under considerations. Lastly Figure 21 shows the results obtained for all the three designs under considerations at a glance.

Fig. 15: Breaking point of carbon fiber (top 4 layers bottom 2 layers) sandwich composite

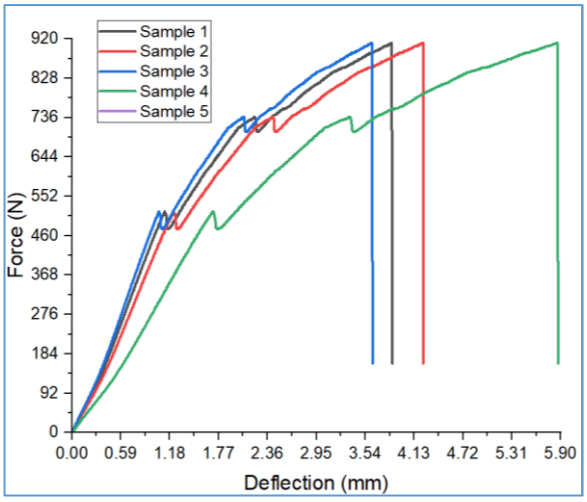

Fig. 16: Force Vs Deflection for Carbon fiber composite (4 Layers at top and 2 layers at bottom)

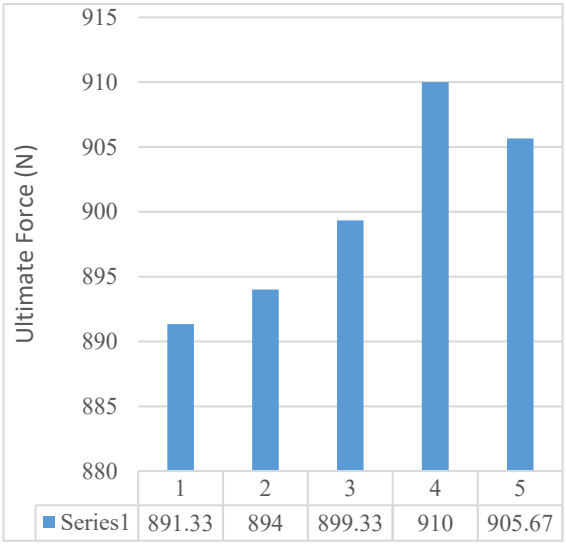

Fig. 17: Ultimate Force of all 5 Samples of carbon fiber composite (4 Layers at top and 2 layers at bottom)

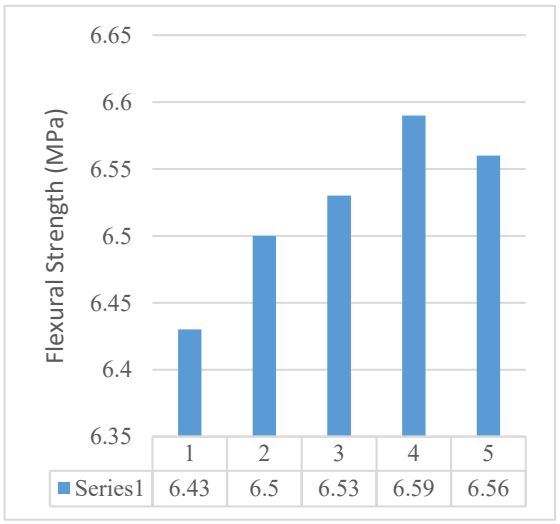

Fig. 18: Flexural strength of all 5 Samples of carbon fiber composite (4 Layers at top and 2 layers at bottom)

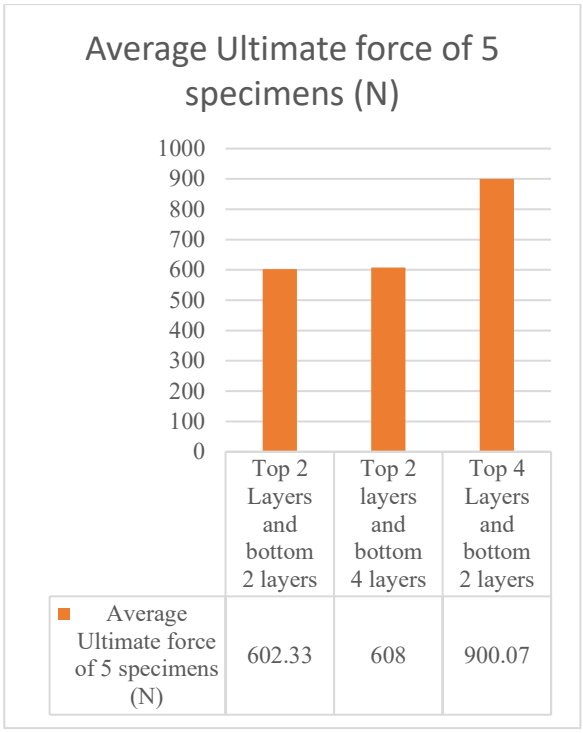

Fig. 19: Comparison between 3 different Symmetry of Carbon fiber sandwich composite in transverse direction

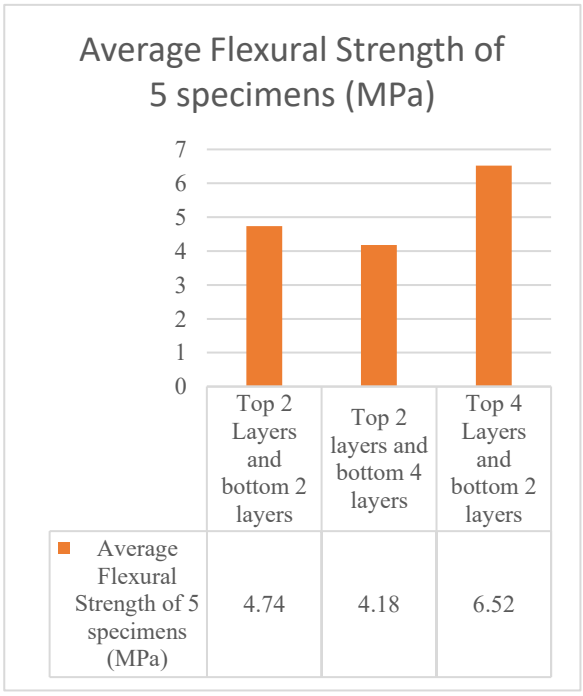

Fig. 20: Comparison between 3 different Symmetry of Carbon fiber sandwich composite in transverse direction

4.6. Differential Scanning Calorimetry (DSC):

This method precisely measures the exothermic energy release (ΔH in J/g) during crosslinking reactions, while identifying critical curing parameters including onset temperature, peak reaction temperature, and reaction completion point. The crosslinking reaction is a poly addition or condensation polymerization where the

functional groups of the resin (epoxide rings) react with the functional groups of the hardener (amine). This forms a dense, three-dimensional, and irreversible covalent network, transforming the low-viscosity liquid mixture into a rigid, thermoset solid with high mechanical strength and thermal stability.

It provides essential data for formulating and optimizing curing processes of thermosetting polymers like epoxy resins, adhesives, and composite matrices. The standard establishes rigorous baseline correction protocols and measurement criteria to ensure reproducibility in evaluating material reactivity and curing kinetics.

It is particularly valuable for optimizing curing cycles, validating resin-hardener formulations, and ensuring batch-to-batch consistency in industrial applications. By adhering to ASTM E2160, manufacturers can precisely control curing parameters, assess reactivity, and predict material behaviour under thermal processing conditions.

For comprehensive analysis, this standard is often paired with ASTM D3418 (Tg determination) to fully characterize a material's thermal properties.

The DSC analysis of the carbon fiber/epoxy composite reveals a well-defined exothermic curing reaction between 88.88°C and 106.92°C of peak at 99.17°C (Tg), indicating efficient epoxy crosslinking with a fast reaction rate and complete cure, characteristic of a properly formulated resin system as shown in Figure 22. These results are crucial for optimizing manufacturing parameters, confirming the resin's cure profile is suitable for processes like autoclave curing (90-110°C range), and ensuring material quality, though additional testing to higher temperatures is recommended to fully characterize the thermal properties, including Tg determination and assessment of thermal stability.

The DSC analysis of the liquid epoxy system (EP 5052) reveals a well-defined exothermic curing reaction with an onset temperature of 49.13°C, peak at 77.22°C, and completion by 122.48°C, indicating a low temperature curing profile suitable for applications requiring mild processing conditions. The enthalpy of 439.7 J/g reflects the total energy released during crosslinking, suggesting a highly reactive resin-hardener combination (100:38 ratio). The sharp, single exothermic peak confirms efficient and homogeneous curing without side reactions, while the relatively low peak temperature (77.22°C) implies minimal thermal stress during processing as shown in Figure 23.

The DSC graph of the carbon fiber-reinforced epoxy composite shows a clear exothermic curing reaction (positive heat flow) beginning around 50°C, peaking near 150°C, and completing by 200°C, with a total enthalpy (heat of reaction) estimated from the peak area referred from Figure 24. The broad exotherm suggests a controlled curing process typical of epoxy systems, where heat release is distributed over a wide temperature range (150°C span), likely due to the resin's complex crosslinking kinetics or fiber-matrix interactions.

The absence of endothermic peaks (negative heat flow) rules out melting or degradation in this range, while the smooth baseline after 200°C indicates complete curing.

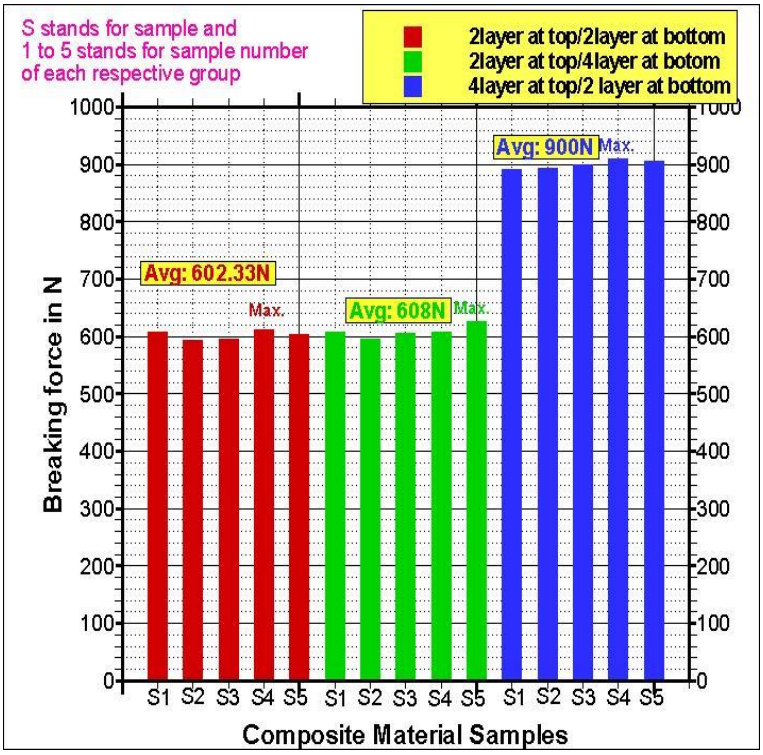

Fig. 21: Experimental results on all the three face sheet stacking sequences i.e. 2/2, 2/4-, and 4/2-layers top/bottom respectively

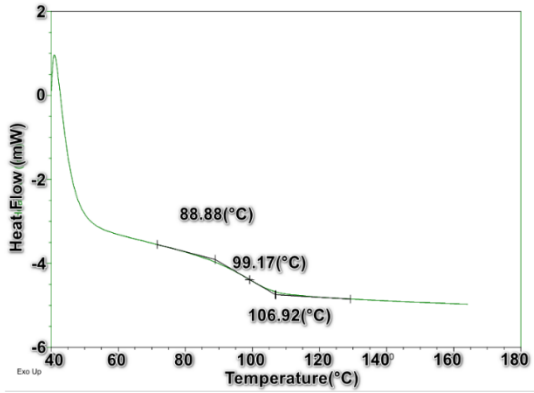

Fig. 22: Carbon Fiber reinforcement with epoxy resin cure Tg run

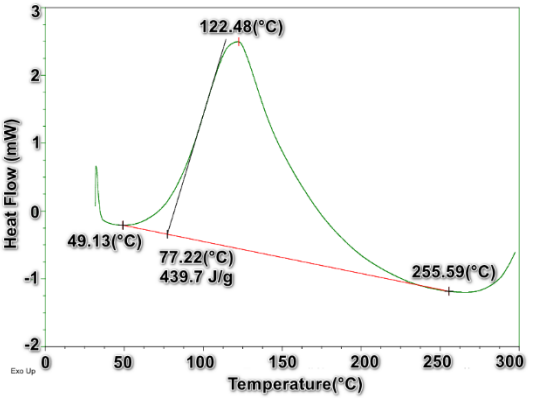

Fig. 23: EP 5052 (Epoxy resin) Liquid enthalpy graph

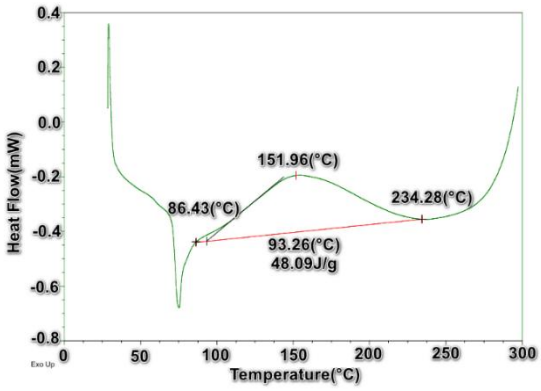

Fig. 24: Carbon reinforcement with epoxy cure Enthalpy graph

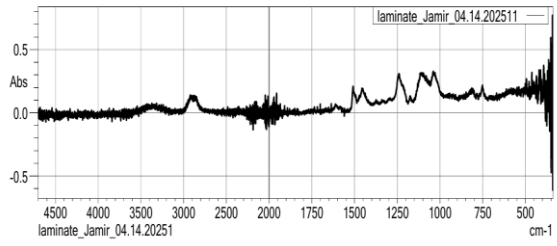

Fig. 25: FT-IR results of Carbon Epoxy laminate

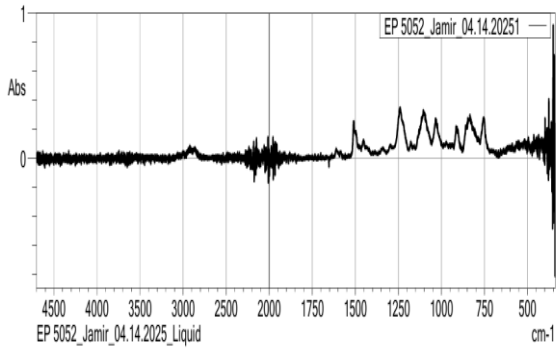

Fig. 26: FT-IR result of uncured liquid resin

4.7. FT-IR (Fourier Transform Infrared Spectroscopy)

The resulting spectrum is plotted as absorbance or transmittance versus wavenumber or wavelength, allowing scientists to interpret the composition and structure of the sample.

4.7.1. Epoxy Resin Dominance:

The library matches (Scores 747–657) strongly indicate the presence of epoxy resins, with multiple entries for epoxy adhesives and epoxy resins used in electronic parts. This suggests the sample is likely an epoxy-based material, such as a laminate or adhesive as shown in Figure 25.
Characteristic epoxy peaks in FTIR typically include:
915 cm^{-1}: Epoxy ring vibration (C-O-C stretch).
1240 cm^{-1} and 1030 cm^{-1}: Aromatic ether (C-O) stretches.
1500–1600 cm^{-1}: Aromatic ring vibrations (C=C).
Broad 3400 cm^{-1}: O-H stretch (if uncured or hydrated).

4.7.2. Phenoxy Resin and Bisphenol A:

Matches for phenoxy resin (Score 674) and bisphenol A (Score 649) suggest these may be components or precursors in the epoxy formulation. Bisphenol A is a common monomer in epoxy resin synthesis.

4.7.3. Ethylene/Vinyl Acetate (EVA) Copolymer:

Lower-score matches (Scores 632–627) indicate trace or secondary components like EVA (ethylene/vinyl acetate), which might be present as a modifier or contaminant. EVA peaks include:
1740 cm^{-1}: C=O stretch (acetate group).
^{1}: C-O stretch (acetate).
The FTIR result shown in Figure 26 indicate a strong presence of epoxy resin, supported by high library match scores (761–665), with key peaks likely corresponding to epoxy functional groups such as C-O-C stretch (915 cm^{-1}) and aromatic rings (1500–1600 cm^{-1}). Secondary matches include phenoxy resin, bisphenol A (a common epoxy precursor).

4.8. SEM (Scanning Electron Microscope)

The SEM images of the carbon fiber sandwich composite reveal a well-organized, tightly packed unidirectional fiber

Cite: J. Havaldar et al., "Optimization of Unidirectional Carbon/Epoxy Facesheets for Enhanced Flexural Strength in PVC Foam Sandwich Beam". Evergreen, 13 (01) 307-327 (2026). https://doi.org/10.5109/7411077.

architecture, indicating precise layup and effective structural alignment crucial for high mechanical performance. The fiber diameters, consistently around 5.8 to 7.9 µmas shown in Figure 27, Figure 29 and Figure 31. It confirms the use of high-quality carbon fibers. The SEM Figure 28, Figure 30 and Figure 32 reveal significant microstructural features and failure mechanisms typical of brittle materials. Clear evidence of fiber rupture indicates sudden and catastrophic failure, which is characteristic of carbon fibers due to their high stiffness and low elongation capacity. The presence of fiber-matrix debonding and matrix cracks highlights interfacial weaknesses and stress concentration points that contribute to the overall failure of the composite. Additionally, dispersed epoxy matrix regions suggest localized matrix damage and potential issues in resin distribution or bonding. The smooth, sharp-edged carbon fibers with consistent diameters confirm the use of high-quality reinforcement. Overall, the images reflect the brittle nature of carbon fibers, which, while offering excellent strength and stiffness, fail abruptly without significant deformation, emphasizing the need for careful structural design in applications where toughness and gradual failure are critical.

Carbon fibers are known for their high strength and stiffness, but they also exhibit brittle failure behaviour. Unlike ductile materials, which deform plastically before failure, carbon fibers can withstand high loads up to a certain point, beyond which they fail suddenly and catastrophically with little or no warning. This is clearly observed in the SEM images of carbon fiber sandwich composites, where fiber rupture appears clean and abrupt, indicating a brittle fracture mechanism. The failure occurs once the tensile or shear stress exceeds the fiber's ultimate strength, without significant elongation or plastic deformation. This characteristic makes carbon fiber composites ideal for high-performance applications requiring lightweight yet strong materials, such as aerospace, automotive, and sporting goods. However, it also means that design safety margins must be carefully considered, as failure tends to be sudden and complete, with little tolerance for overloading or impact.

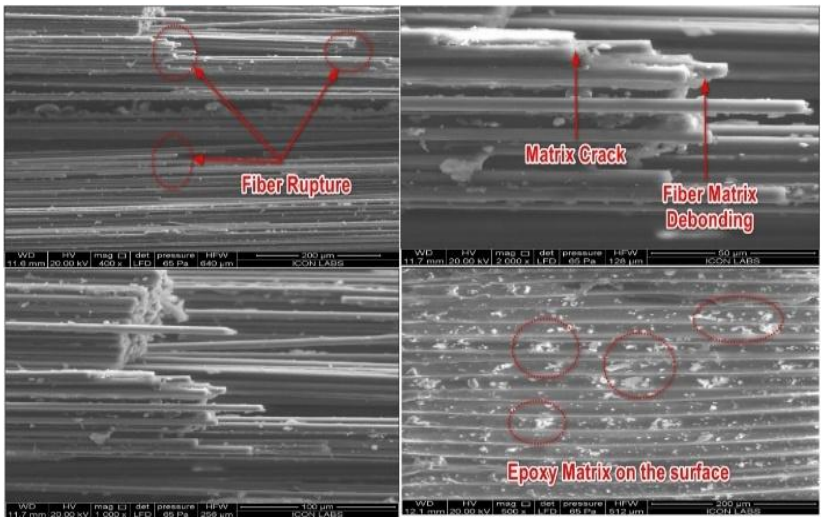

Fig. 27: SEM image of Carbon Fiber reinforced sandwich composite (Fibers aligned in Transverse direction 2 layers at top and 2 Layers at bottom)

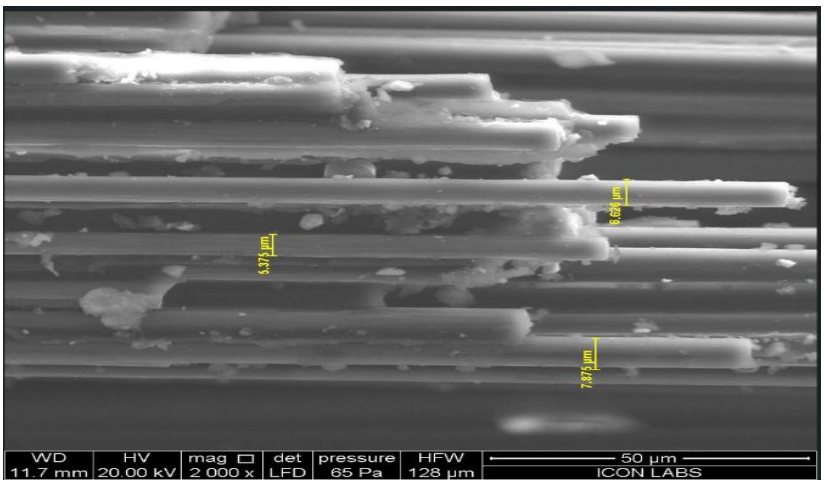

Fig. 28: Diameter of single Carbon Filament

Cite: J. Havaldar et al., "Optimization of Unidirectional Carbon/Epoxy Facesheets for Enhanced Flexural Strength in PVC Foam Sandwich Beam". Evergreen, 13 (01) 307-327 (2026). https://doi.org/10.5109/7411077.

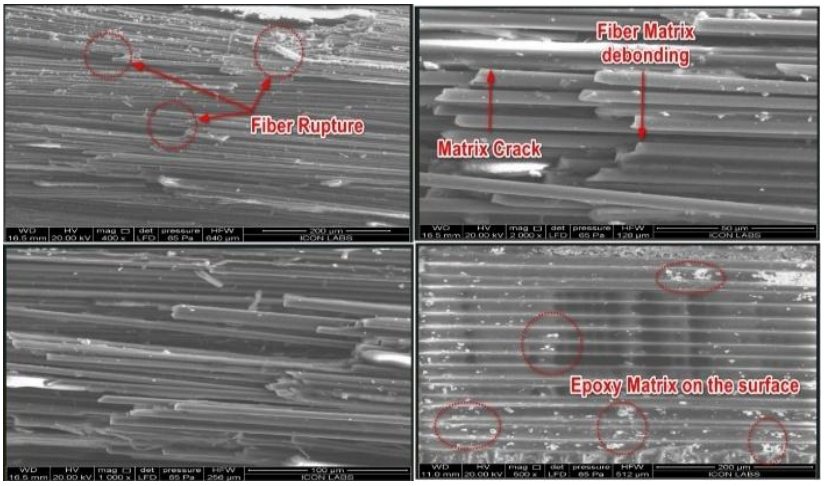

Fig. 29: SEM image of Carbon fiber reinforced sandwich composite (Fibers aligned in Transverse direction 2 layers at top and 4 Layers at bottom)

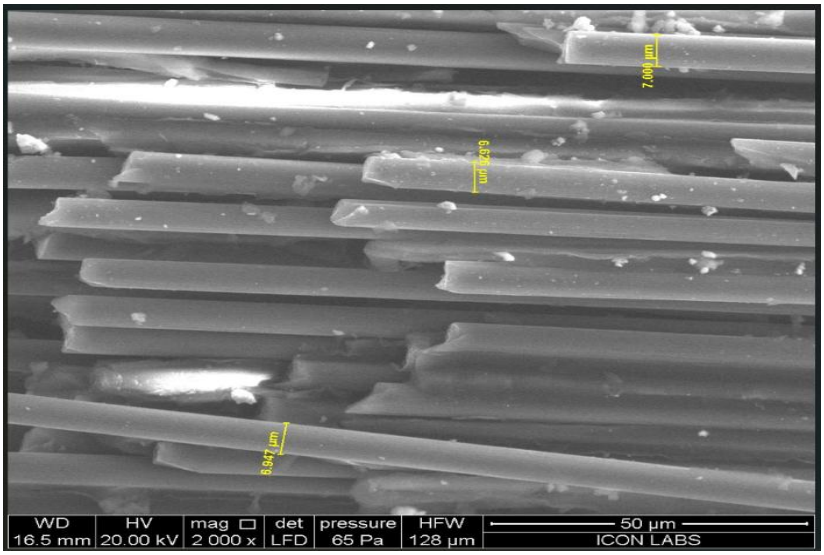

Fig. 30: Diameter of Single Carbon Filament

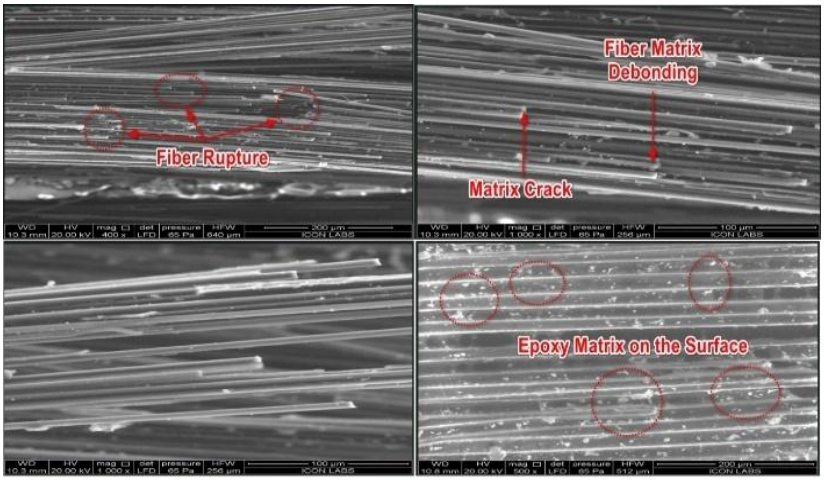

Fig. 31: SEM image of Carbon Fiber reinforced sandwich composite (Fibers aligned in Transverse direction 4 layers at top and 2 Layers at bottom)

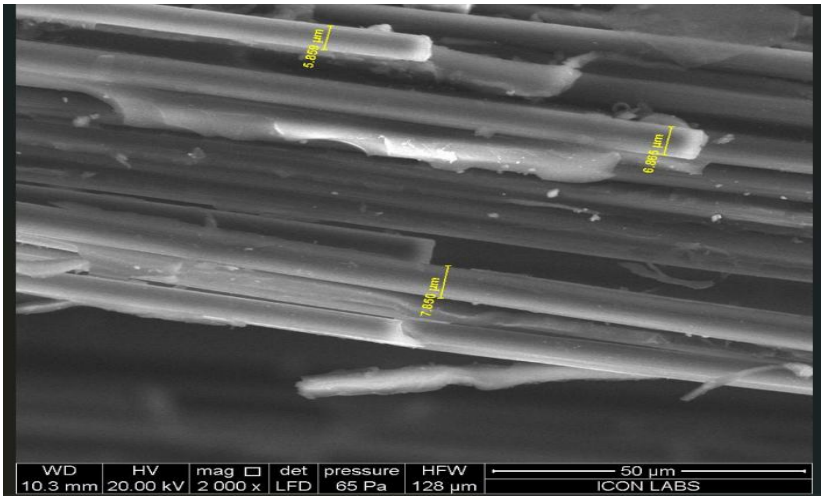

Fig. 32: Diameter of Single Carbon Filament

4.9. Energy-Dispersive X-ray Spectroscopy (EDS or EDX):

The study shows the EDS results of carbon fiber composites at rupture region and at surface of composite. The basic idea of this is to see the elemental composition at two different region i.e at rupture region and at surface of composite materials. The EDAX APEX analysis this sample reveals a high carbon content (~95-96.5 wt%) with minor oxygen (~3.5-4.6 wt%) across three selected areas as shown in Figure 33. Area 2 shows trace chlorine (0.2 wt%), suggesting potential contamination or residue. The atomic percentages align closely, with carbon dominating (~96-97 at%). Net intensities for carbon are significantly higher (1239-1592.9 counts) compared to oxygen (29.7-34.5 counts) and chlorine (20.4 counts). The consistent high carbon concentration indicates a carbon-rich material, possibly graphite or a polymer, with minimal oxidation. The presence of chlorine is due to the core material of Polyvinyl chloride. Overall, the material is predominantly carbon with minor oxygen incorporation.

The EDAX APEX analysis of sample shows a carbon-rich surface with ~82-83 wt% carbon and ~16-17 wt% oxygen across three selected areas as shown in Figure 34. Atomic percentages confirm carbon dominance (~86-87 at%) with lower oxygen (~12-13 at%). Area 3 reveals trace chlorine (1.1 wt%), likely indicating contamination or residue. Net intensities for carbon (1010.8-1426.4 counts) are higher than oxygen (144.4-209.9 counts) and chlorine (114.3 counts). The elevated oxygen content compared to the rupture region suggests surface oxidation or organic contamination. The material remains carbon-dominated with notable oxygen incorporation.

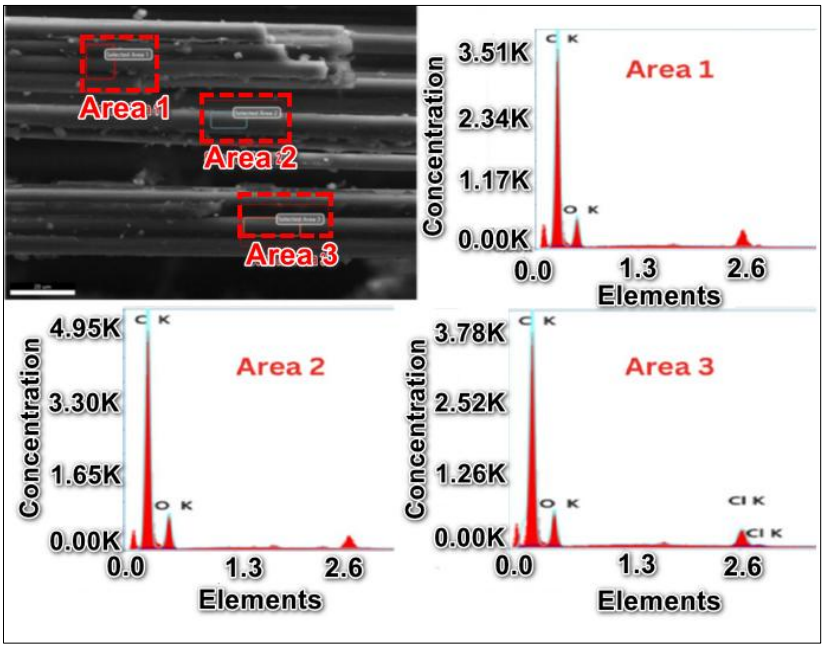

Fig. 33: EDS results of Carbon Fiber sandwich composite (2 Layers at top and 4 Layers at bottom) at rupture region

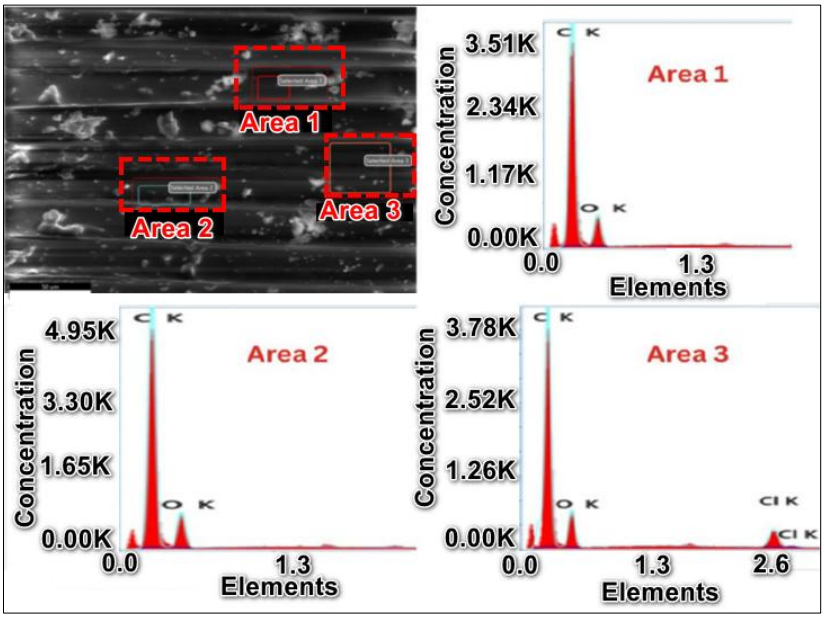

Fig. 34: EDS results of Carbon Fiber sandwich composite (2 Layers at top and 2 Layers at bottom) at surface

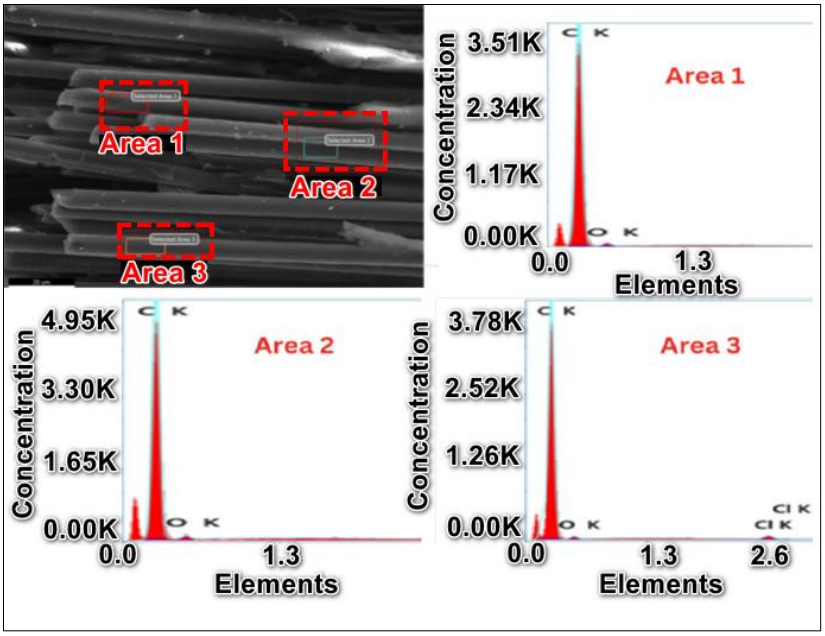

Fig. 35: EDS results of Carbon Fiber sandwich composite (2 Layers at top and 4 Layers at bottom) at rupture region

The EDAX APEX analysis of sample reveals an exceptionally high carbon content (~97.2–97.6 wt%) with minimal oxygen (~2.2–2.8 wt%) across three selected areas as shown in Figure 35. Atomic percentages confirm carbon dominance (~97.9–98.2 at%), indicating a near-pure carbon material, likely graphite or a similar carbon-based structure. Trace chlorine (0.3 wt%) appears in Area 3, suggesting minor contamination. Net intensities for carbon (651.9–1086.5 counts) far exceed oxygen (9.7–14.0 counts) and chlorine (21.5 counts), this material exhibits higher carbon purity and lower oxygen content, implying superior structural integrity or reduced environmental exposure. The results highlight a highly carbon-rich composition with negligible impurities The EDAX APEX analysis of sample reveals a carbon-rich surface (~81.9–82.0 wt%) with significant oxygen content (~16.9–18.1 wt%), consistent across three selected areas as shown in Figure 36. Atomic percentages show carbon dominance (~85.7–86.2 at%) but with higher oxygen (~13.4–14.3 at%). Area 3 detects trace chlorine (1.1 wt%), suggesting surface contamination due to PVC core. Net intensities for carbon (1180.8–1309.2 counts) exceed oxygen (194.7–211.9 counts) and chlorine (137.3 counts). The elevated oxygen levels indicate surface oxidation or organic residues, likely from environmental exposure. The material remains carbon-dominated but with notable

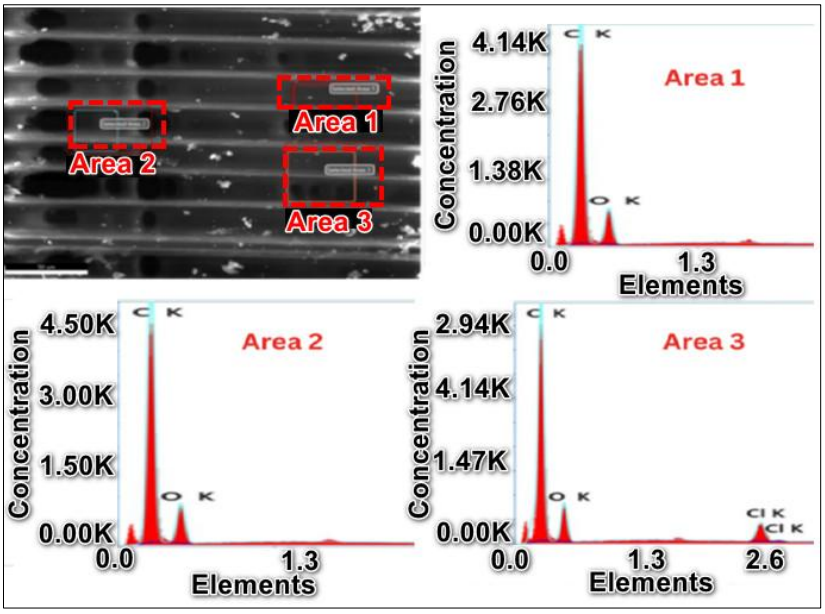

Fig. 36: EDS results of Carbon Fiber sandwich composite (2 Layers at top and 4 Layers at bottom) at surface

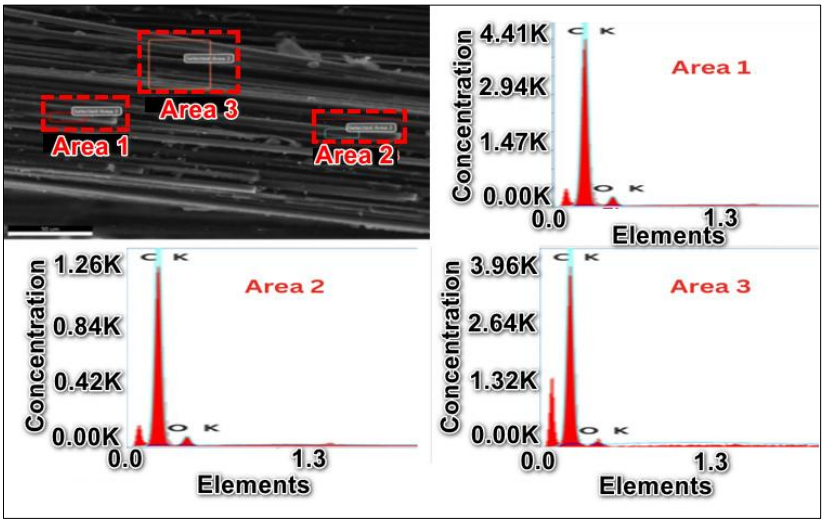

Fig. 37: EDS results of Carbon Fiber sandwich composite (4 Layers at top and 2 Layers at bottom) at rupture region

oxygen incorporation on the surface.

The EDAX APEX analysis of sample shows a high carbon content (~92.1–96.6 wt%) with minor oxygen (~3.4–7.9 wt%) across three selected areas as shown in Figure 37. Atomic percentages confirm carbon dominance (~94.0–97.4 at%), indicating a primarily carbon-based material, such as graphite or carbon fiber. Net intensities for carbon (367.2–1301.6 counts) are significantly higher than oxygen (6.8–64.3 counts), reflecting the material's carbon-rich nature. Area 3 exhibits the highest carbon purity (96.6 wt%) and lowest oxygen (3.4 wt%), suggesting localized variations in composition. The results align with typical carbon materials but show slightly higher oxygen content compared to ultra-pure carbon forms, possibly due to surface oxidation or minor impurities. Overall, the sample is predominantly carbon with minimal oxygen incorporation.

The EDAX APEX analysis reveals a carbon-rich surface (82.7–84.5 wt%) with significant oxygen content (15.5–16.7 wt%) across three selected areas as shown in Figure 38. Atomic percentages show carbon dominance (86.8–87.9 at%) but with notable oxygen incorporation (12.1–13.1 at%). Area 3 detects trace chlorine (1.0 wt%), likely indicating surface contamination. Net intensities for carbon (856.3–1118.4 counts) exceed oxygen (108.3–158.1 counts) and chlorine (90.3 counts), the surface exhibits higher oxygen levels, suggesting oxidation or organic residues from environmental exposure. The results highlight a carbon-dominated surface with measurable oxygen and minor chlorine impurities.

Past studies focus on sandwich panels with glass/epoxy skins and polyurethane/phenolic foam cores, fabricated using hand lay-up. Only two fiber orientations (balance symmetry and quasi-isotropic) are tested. The author

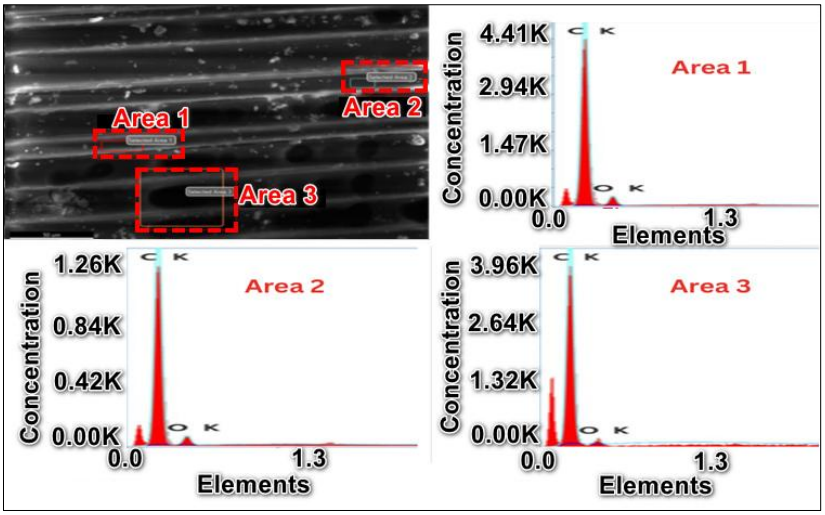

Fig. 38: EDS results of Carbon Fiber sandwich composite (4 Layers at top and 2 Layers at bottom) at surface

introduces carbon fiber/epoxy composite with PVC cores, fabricated via vacuum infusion. The author adds three configurations (2/2, 2/4, and 4/2 layers). This adds 3 unique material variants, significantly broadening the study. Past studies is limited to 4-point bending tests under static loading, with comparisons between experimental and analytical results for flexural stiffness and deflection. Failure modes are briefly discussed. The author expands testing to detailed 4-point bending results for all material configurations, including ultimate force, deflection and ultimate flexural strength. Differential Scanning Calorimetry (DSC) to analyse curing behaviour (Tg, enthalpy) of epoxy resins, adhering to ASTM E2160. FT-IR spectroscopy to characterize chemical composition of cured/uncured resins, referencing ASTM E168/E1252. Visual documentation in the form of Scanning electron microscopy (SEM) of failure modes (delamination, cracking) for each configuration, with images and graphs. The past results and discussion present, tabulated data for flexural stiffness and deflection, with limited graphical representation (e.g., Load vs. Deflection curves for PU/phenolic cores) but got highest values up to 6kN as per ASTM D 7250.The author conducted the test as per ASTM D 5467 and got the highest values of 900N. The author adds Carbon fiber composites and PVC cores, which is not conducted or studied till now. The author significantly extends the work by introducing new materials, advanced fabrication methods, and additional analytical techniques. It provides a more comprehensive dataset (mechanical, thermal, chemical) and detailed failure analysis, making it a substantial expansion of the original study. The past studies focus on flexural behaviour of foam-core sandwiches is preserved, but the author adds multi-layered composites, curing kinetics, and molecular characterization, enhancing both practical and theoretical insights.

5. Conclusion

This study explored the optimization of carbon fiber-reinforced polymer matrix composite (PMC) sandwich beams by varying the number of carbon fiber layers in the facesheets to improve flexural strength. Using a vacuum infusion process with PVC foam as the core, three configurations (2/2, 2/4- and 4/2-layers top/bottom) were fabricated and tested under 4-point bending according to ASTM D5467. Among the tested configurations, the 4-top/2-bottom layer setup exhibited the highest flexural performance, achieving a peak load of 910 N and an average strength of 900.07 N. The investigation into three carbon fiber-epoxy and PVC foam configurations revealed a clear performance hierarchy based on layer distribution. The symmetrical 2/2 top/bottom setup provided a baseline strength of 602.33 N, while the asymmetrical 2/4 top/bottom version showed a negligible improvement to 608 N, indicating that reinforcing only the bottom face was ineffective. In stark contrast, the inverse 4/2 top/bottom configuration achieved a dramatically higher load capacity of 900 N, conclusively demonstrating that placing more layers on the top face was the optimal design for maximizing strength under the tested conditions. Force-deflection and strain analysis indicated that increasing the top facesheet thickness significantly enhances the beam's ability to carry load and dissipate energy before failure. This configuration also showed a more gradual and progressive failure mode compared to the abrupt brittle failure observed in the symmetric 2/2 configuration.

To further validate the mechanical findings, a series of complementary characterization techniques were employed. Differential Scanning Calorimetry (DSC) was conducted to assess the curing behaviour of the epoxy resin system, confirming that the curing process was both complete and highly efficient, ensuring optimal cross-linking and thermal stability. Additionally, Fourier

Transform Infrared Spectroscopy (FT-IR) was utilized to analyze the chemical composition of the composite, clearly identifying the characteristic functional groups of the epoxy matrix as well as trace amounts of resin additives, which play a crucial role in enhancing material properties. Microstructural evaluation was performed using Scanning Electron Microscopy (SEM), which provided high-resolution images of the composite's fracture surfaces. These images revealed that fiber rupture and matrix cracking were the dominant failure mechanisms, indicating stress concentration points and interfacial bonding characteristics between the fibers and the matrix. To complement SEM observations, Energy Dispersive X-ray Spectroscopy (EDS) was employed to determine the elemental composition of the composite. The EDS analysis confirmed that the material was primarily carbon-rich, consistent with the carbon fiber reinforcement, while also detecting minor surface oxidation and residual polyvinyl chloride (PVC) particles, which may have influenced interfacial adhesion and overall durability.

The integration of these analytical techniques provided a comprehensive understanding of the composite's structural integrity and failure behaviour. The findings underscore the importance of optimizing layer distribution in carbon fiber sandwich beams, as it directly impacts load-bearing capacity, flexural rigidity, and energy absorption. By carefully tailoring the stacking sequence and resin formulation, it is possible to achieve a superior balance between lightweight design and mechanical strength.

This study highlights the potential of advanced composite materials in high-performance applications, particularly in industries such as aerospace, where weight reduction is critical, and automotive and civil engineering, where structural efficiency and durability are paramount. Future research could explore the effects of alternative resin systems, hybrid reinforcements, and environmental aging on long-term performance, further enhancing the applicability of these materials in real-world scenarios.

6. Future scope:

Future research could explore the use of advanced core materials such as Nomex honeycomb, aluminium foam to enhance shear resistance and energy absorption, while also investigating fiber reinforcement of different GSM with increase in layers. Additionally, incorporating nanofillers (e.g., graphene, carbon nanotubes) into the epoxy matrix could improve interfacial bonding and fracture toughness, further enhancing the mechanical performance and damage tolerance of sandwich composites under diverse loading conditions. PVC foam core with carbon fiber facesheets serves as a crucial baseline for future studies. Researchers can directly compare their results using advanced materials like Nomex honeycomb or nanofiller-enhanced epoxies against your findings to quantify the improvements in shear resistance, energy absorption, and fracture toughness.

Conflict of interest

No potential conflict of interest was reported by the author(s).

Discloser of the source of funding for this study

There is no funding provided by any agency for this paper.

Author's contribution

The authors confirm their contribution to the paper: study conception and design: Sachin Solanke and Sachin Shinde. Data collection and Testing of Samples and Drafting of Results Jameer Havaldar.

Nomenclature

ASTM	American Society for Testing and Materials
DSC	Differential Scanning Calorimetry
EDS	Energy Dispersive X-ray Spectroscopy
EP	Epofine (Epoxy resin)
FT-IR	Fourier Transform Infrared Spectroscopy
FH	Fine Hard (Hardener)
GSM	Grams per Square Meter
PVA	Poly-vinyl Alcohol
PVC	Poly-vinyl Chloride
SEM	Scanning Electron Microscope
T_g	Glass Transition Temperature

References

1) C. Borsellino, L. Calabrese, and A. Valenza, "Experimental and numerical evaluation of sandwich composite structures," Compos. Sci. Technol., 64 (10–11) 1709–1715 (2004). doi:10.1016/j.compscitech.2004.01.003.
2) T.H.E. S-version, and F.E. Method, "For laminated," 39 (April) 3641–3662 (1996).
3) M.W. Brown, and K.J. Miller, "High temperature low cycle biaxial," 1 217–229 (1979).
4) W.N. Findley, "A theory for the effect of mean stress on fatigue of metals under combined torsion and axial load or bending," J. Eng. Ind., 81 (4) 301–305 (1959). doi:10.1115/1.4008327.
5) J.S. Huang, and S.Y. Liu, "Fatigue of honeycombs unders in-plane multiaxial loads," Mater. Sci. Eng. A, 308 (1–2) 45–52 (2001). doi:10.1016/S0921-5093(00)01996-1.
6) J.S. Huang, and J.Y. Lin, "Fatigue of cellular materials," Acta Mater., 44 (1) 289–296 (1996). doi:10.1016/1359-6454(95)00170-4.
7) C. Burchardt, "Fatigue in sandwich structures loaded

in transverse shear," Compos. Struct., 40 (1) 73–79 (1997). doi:10.1016/S0263-8223(97)00157-8.

8) J. Hohe, and W. Becker, "Effective stress-strain relations for two-dimensional cellular sandwich cores: homogenization, material models, and properties," Appl. Mech. Rev., 55 (1) 61–87 (2002). doi:10.1115/1.1425394.
9) N. Kulkarni, H. Mahfuz, S. Jeelani, and L.A. Carlsson, "Fatigue failure mechanism and crack growth in foam core sandwich composites under flexural loading," J. Reinf. Plast. Compos., 23 (1) 83–94 (2004). doi:10.1177/0731684404029347.
10) R.A.W. Mines, and A. Alias, "Numerical simulation of the progressive collapse of polymer composite sandwich beams under static loading," 33 11–26 (2002).
11) A. Petras, and M.P.F. Sutcli, "Indentation failure analysis of sandwich beams," 50 311–318 (2000).
12) A.P. Mouritz, and R.S. Thomson, "Compression, flexure and shear properties of a sandwich composite containing defects," Compos. Struct., 44 (4) 263–278 (1999). doi:10.1016/S0263-8223(98)00133-0.
13) L. Vaikhanski, and S.R. Nutt, "Fiber-reinforced composite foam from expandable pvc microspheres," 34 1245–1253 (2003). doi:10.1016/S1359-835X(03)00255-0.
14) H. Lin, "The structure and property relationships of commercial foamed plastics," 9418 (97) 429–443 (1997).
15) E. Bozhevolnaya, and O.T. Thomsen, "Structurally graded core junctions in sandwich beams: fatigue loading conditions," Compos. Struct., 70 (1) 12–23 (2005). doi:10.1016/j.compstruct.2004.08.029.
16) G. Belingardi, "Material characterization of a composite – foam sandwich for the front structure of a high speed train," 61 13–25 (2003). doi:10.1016/S0263-8223(03)00028-X.
17) B. Freeman, E. Schwingler, M. Mahinfalah, and K. Kellogg, "The effect of low-velocity impact on the fatigue life of sandwich composites," Compos. Struct., 70 (3) 374–381 (2005). doi:10.1016/j.compstruct.2004.09.027.
18) E.E. Gdoutos, I.M. Daniel, and K. Wang, "Compression facing wrinkling of composite sandwich structures," 35 511–522 (2003).
19) V.S. Sokolinsky, H. Shen, L. Vaikhanski, and S.R. Nutt, "Experimental and analytical study of nonlinear bending response of sandwich beams," 60 219–229 (2003). doi:10.1016/S0263-8223(02)00293-3.
20) B.K. Hadi, and F.L. Matthews, "Development of benson ± mayers theory on the wrinkling of anisotropic sandwich panels," 49 425–434 (2000).
21) R.A.W. Mines, and A.G. Gibson, "LOW velocity perforation behaviour of polymer composite sandwich panels," 21 (10) 855–879 (1998).
22) L. Torre, and J.M. Kenny, "Impact testing and simulation of composite sandwich structures for civil transportation," 50 257–267 (2000).
23) G. Kalaprasad, P. Pradeep, G. Mathew, C. Pavithran, and S. Thomas, "Thermal conductivity and thermal di usivity analyses of low-density polyethylene composites reinforced with sisal , glass and intimately mixed sisal / glass ® bres," 60 2967–2977 (2000).
24) S. Sahraoui, E. Mariez, and M. Etchessahar, "Mechanical testing of polymeric foams at low frequency," 20 93–96 (2001).
25) C.A. Steeves, and N.A. Fleck, "Collapse mechanisms of sandwich beams with composite faces and a foam core , loaded in three-point bending . part i : analytical models and minimum weight design," 46 561–583 (2004). doi:10.1016/j.ijmecsci.2004.04.003.
26) M. Danielsson, J.L. Grenestedt, and D.I. Ab, "Gradient foam core materials for sandwich structures : preparation and characterisation," (97) 981–988 (1998).
27) S.D. Clark, R.A. Shenoi, and H.G. Allen, "Modelling the fatigue behaviour of sandwich beams under monotonic, 2-step and block-loading regimes," Compos. Sci. Technol., 59 (4) 471–486 (1999). doi:10.1016/S0266-3538(98)00088-8.
28) .B Ashforth, and .B Ashforth, "From the sage social science collections . rights reserved .," Ann. Am. Acad. Pol. Soc. Sci., 503 (1) 122–136 (1986).
29) W. Becker, "Closed-form analysis of the thickness effect of regular honeycomb core material," Compos. Struct., 48 (1) 67–70 (2000). doi:10.1016/S0263-8223(99)00074-4.
30) H. Judawisastra, J. Ivens, and I. Verpoest, "The fatigue behaviour and damage development of 3d woven sandwich composites," Compos. Struct., 43 (1) 35–45 (1998). doi:10.1016/S0263-8223(98)00093-2.
31) J.N. Yang, D.L. Jones, S.H. Yang, and A. Meskini, "A stiffness degradation model for graphite/epoxy laminates," J. Compos. Mater., 24 (7) 753–769 (1990). doi:10.1177/002199839002400705.
32) E. REISSNER, "Finite deflections of sandwich plates," J. Aeronaut. Sci., 15 (7) 435–440 (1948). doi:10.2514/8.11610.
33) J.M. Albuquerque, M.F. Vaz, and M.A. Fortes, "Effect of missing walls on the compression behaviour of honeycombs," Scr. Mater., 41 (2) 167–174 (1999). doi:10.1016/S1359-6462(99)00117-7.
34) J. Hinczica, M. Messiha, T. Koch, A. Frank, and G. Pinter, "Influence of recyclates on mechanical properties and lifetime performance of polypropylene materials," Procedia Struct. Integr., 42 (2019) 139–146 (2022). doi:10.1016/j.prostr.2022.12.017.

35) N.K. Bau-Madsen, K.H. Svendsen, and A. Kildegaard, “Large deflections of sandwich plates - an experimental investigation,” Compos. Struct., 23 (1) 47–52 (1993). doi:10.1016/0263-8223(93)90073-Y.
36) M. Doyoyo, and D. Mohr, “Microstructural response of aluminum honeycomb to combined out-of-plane loading,” Mech. Mater., 35 (9) 865–876 (2003). doi:10.1016/S0167-6636(02)00308-3.
37) S.D. Pan, L.Z. Wu, Y.G. Sun, Z.G. Zhou, and J.L. Qu, “Longitudinal shear strength and failure process of honeycomb cores,” Compos. Struct., 72 (1) 42–46 (2006). doi:10.1016/j.compstruct.2004.10.011.
38) M.Y. Yang, and J.S. Huang, “Elastic buckling of regular hexagonal honeycombs with plateau borders under biaxial compression,” Compos. Struct., 71 (2) 229–237 (2005). doi:10.1016/j.compstruct.2004.10.014.
39) W. Hwang, and K.S. Han, “Fatigue of composites—fatigue modulus concept and life prediction,” J. Compos. Mater., 20 (2) 154–165 (1986). doi:10.1177/002199838602000203.
40) C. Caglayan, I. Gurkan, S. Gungor, and H. Cebeci, “The effect of cnt-reinforced polyurethane foam cores to flexural properties of sandwich composites,” Compos. Part A Appl. Sci. Manuf., 115 187–195 (2018). doi:10.1016/j.compositesa.2018.09.019.
41) Q. Chen, T. Linghu, Y. Gao, Z. Wang, Y. Liu, R. Du, and G. Zhao, “Mechanical properties in glass fiber pvc-foam sandwich structures from different chopped fiber interfacial reinforcement through vacuum-assisted resin transfer molding (vartm) processing,” Compos. Sci. Technol., 144 202–207 (2017). doi:10.1016/j.compscitech.2017.03.033.
42) S. Mudassir, D.V.R. Shankar, and M.M. Hussain, “Flexural behavior of sandwich composite panels under 4-point loading,” Int. J. Mater. Sci., 11 (1) 47–55 (2016). http://www.ripublication.com.
43) I.M. Daniel, and J.L. Abot, “Fabrication, testing and analysis of composite sandwich beams,” Compos. Sci. Technol., 60 (12–13) 2455–2463 (2000). doi:10.1016/S0266-3538(00)00039-7.
44) A. Russo, and B. Zuccarello, “Experimental and numerical evaluation of the mechanical behaviour of gfrp sandwich panels,” Compos. Struct., 81 (4) 575–586 (2007). doi:10.1016/j.compstruct.2006.10.007.
45) J. Kim, and S.R. Swanson, “Design of sandwich structures for concentrated loading,” 52 365–373 (2001).
46) K. Kanny, and H. Mahfuz, “Flexural fatigue characteristics of sandwich structures at different loading frequencies,” Compos. Struct., 67 (4) 403–410 (2005). doi:10.1016/j.compstruct.2004.01.021.
47) A.M. Harte, N.A. Fleck, and M.F. Ashby, “The fatigue strength of sandwich beams with an aluminium alloy foam core,” Int. J. Fatigue, 23 (6) 499–507 (2001). doi:10.1016/S0142-1123(01)00012-3.
48) E.M. Reis, and S.H. Rizkalla, “Material characteristics of 3-d frp sandwich panels,” Constr. Build. Mater., 22 (6) 1009–1018 (2008). doi:10.1016/j.conbuildmat.2007.03.023.
49) S. Belouettar, A. Abbadi, Z. Azari, R. Belouettar, and P. Freres, “Experimental investigation of static and fatigue behaviour of composites honeycomb materials using four point bending tests,” Compos. Struct., 87 (3) 265–273 (2009). doi:10.1016/j.compstruct.2008.01.015.
50) A. Kootsookos, and P.J. Burchill, “The effect of the degree of cure on the corrosion resistance of vinyl ester / glass fibre composites,” 35 501–508 (2004). doi:10.1016/j.compositesa.2003.08.010.
51) Lin Ye, “Role of matrix resin in delamination onset and growth in composite laminates,” Compos. Sci. Technol., 33 (4) 257–277 (1988). doi:10.1016/0266-3538(88)90043-7.
52) Y.M. Jen, and L.Y. Chang, “Evaluating bending fatigue strength of aluminum honeycomb sandwich beams using local parameters,” Int. J. Fatigue, 30 (6) 1103–1114 (2008). doi:10.1016/j.ijfatigue.2007.08.006.
53) G. Demelio, K. Genovese, and C. Pappalettere, “An experimental investigation of static and fatigue behaviour of sandwich composite panels joined by fasteners,” Compos. Part BEngineering, 32 (4) 299–308 (2001). doi:10.1016/S1359-8368(01)00007-5.
54) W.S. Kuo, J. Fang, and H.W. Lin, “Failure behavior of 3d woven composites under transverse shear,” Compos. Part A Appl. Sci. Manuf., 34 (7) 561–575 (2003). doi:10.1016/S1359-835X(03)00123-4.
55) ASTM D5467, “Standard test method for compressive properties of unidirectional polymer matrix composite materials using a sandwich beam,” ASTM Stand., 97 (Reapproved) 1–9 (2010). doi:10.1520/D5467.
56) G. Liu, and H. Liu, “Thin-walled structures synergistic design of curved beam metastructures with tunable stiffness , poisson ’ s ratio and energy absorption ability,” Thin-Walled Struct., 218 (PA) 113938 (2026). doi:10.1016/j.tws.2025.113938.
57) M. Burman, and D. Zenkert, “Fatigue of foam core sandwich beams - 2: effect of initial damage,” Int. J. Fatigue, 19 (7) 563–578 (1997). doi:10.1016/S0142-1123(97)00068-6.
58) H. Hu, S. Belouettar, E.M. Daya, and M. Potier-Ferry, “Evaluation of kinematic formulations for viscoelastically damped sandwich beam modeling,” J. Sandw. Struct. Mater., 8 (6) 477–495 (2006). doi:10.1177/1099636206065872.
59) G.S.A.P. TONG, “Pergamon equivalent transverse

honeycomb shear stiffness cores," Int. J. Solids Struct., 32 (10) 1383–1393 (1995).

60) A.K. Noor, W.S. Burton, and C.W. Bert, "Computational models for sandwich panels and shells," Appl. Mech. Rev., 49 (3) 155–199 (1996). doi:10.1115/1.3101923.
61) F. Meraghni, F. Desrumaux, and M.L. Benzeggagh, "Mechanical behaviour of cellular core for structural sandwich panels," Compos. Part A Appl. Sci. Manuf., 30 (6) 767–779 (1999). doi:10.1016/S1359-835X(98)00182-1.
62) C.F.C. Adherends, "Bond parameters to improve tensile load," J. Compos. Mater., 37 (5) (2003). doi:10.1106/002199803031040.
63) F. Bahari-Sambran, R. Eslami-Farsani, and S. Arbab Chirani, "The flexural and impact behavior of the laminated aluminum-epoxy/basalt fibers composites containing nanoclay: an experimental investigation," J. Sandw. Struct. Mater., 22 (6) 1931–1951 (2020). doi:10.1177/1099636218792693.
64) S.G. Solanke, and V.R. Gaval, "Optimization of wet sliding wear parameters of titanium grade 2 and grade 5 bioimplant materials for orthopedic application using taguchi method," J. Met. Mater. Miner., 30 (3) 113–120 (2020). doi:10.14456/jmmm.2020.44.
65) "Erratum: effect of multi-walled carbon nanotubes in reinforced hydroxyapatite composite coatings for orthopedic applications (surf. rev. lett. (2025) 32:6 (2340009) doi: 10.1142/s0218625x23400097)," Surf. Rev. Lett., 32 (9) 25920027 (2025). doi:10.1142/S0218625X25920027.
66) S.G. Solanke, V. Gaval, A. Pratap, and M. Pasarkar, "Crystallinity and cell viability in plasma-sprayed hydroxyapatite coatings," J. Tribol., 30 (June) 61–72 (2021).